Journal of Applied Geophysics 206 (2022) 104775

Contents lists available at ScienceDirect

Journal of Applied Geophysics

journal homepage: www.elsevier.com/locate/jappgeo

Geoelectrical approach to establishing conceptual pit limits in a barite deposit

Ranyere Sousa Silva [a,*], Fabiana Pereira Lasmar [b], Erbertt Barros Bezerra [a], Vagner Roberto Elis [b], Antonio Carlos Martins [c], Giorgio de Tomi [a]

[a] Departamento de Engenharia de Minas e Petróleo, Universidade de Sao Paulo, 05508-030, Brazil
[b] Instituto de Astronomia, Geofísica e Ciências Atmosféricas, Universidade de Sao Paulo, 05508-090, Brazil
[c] Centro Universitário das Faculdades Metropolitanas Unidas, 01318-001, Brazil

ARTICLE INFO

Keywords:
Small-scale mining
Barite
Electrical resistivity

ABSTRACT

Small-scale mining faces many challenges, such as the proportionally higher costs related to mineral exploration, the time for the results associated with these activities to become available and the difficulties to dispose of waste throughout the mine life. This paper considers three innovative approaches to address small-scale mining issues: application of the Electrical Resistivity and Induced Polarization geophysical method in a barite deposit, preliminary geological modeling and conceptual pit design. These approaches were tested as an alternative to conventional exploration and exploitation methods for small-scale mining of barite deposits. The methods were applied to a barite deposit and the results allowed for a targeted drilling campaign that provided savings of over 58%, with the reduction of nearly 62% in time and 93% in waste generated by the future mining operation. The proposed approach also allowed for the construction of targeted, smaller pits aimed at the best exploitation of the deposits. Hence, the proposed methodology proved to be a feasible alternative for the mine planning cycle of small-scale barite deposits.

1. Introduction

For any mining activity to be recognized as productive and competitive, geological exploration is required, with a view to improve decision-making during the mining phase. In the earlier stages of a mining project, the scoping study of small-scale deposits is commonly associated with various challenges. Zvarivadza and Nhleko (2018) cite social, environmental, economic, health and safety issues as key-challenges for the small-scale mining sector. Furthermore, this sector frequently faces difficulties to reduce geological uncertainties and to collect information to support decision-making at the conceptual phases of the project.

Costs of geological exploration and, in particular, drilling campaigns, are not commonly borne by small-scale mining enterprises and alternative methods for the determination and characterization of the ore body should be assessed. For instance, Moreira et al. (2016) demonstrates that geophysical investigations can be a useful alternative tool for detection of stratigraphy layers in small-scale deposits with good predictability rates, reducing drilling costs significantly.

According to Martins et al. (2016a, 2016b), geophysics methods can be efficient to determine the thickness of soil layer at the top of the rock bed and to identify the layers of interest. In addition to providing litho-stratigraphic information encompassing long distances and depths, the processing and interpretation of geophysical data allows for the construction of preliminary geological models at reasonable costs (Zarroca et al., 2015). Ganerød et al. (2008) used Ground Penetration Radar (GPR), refractive seismic and 2D resistivity profiling, integrated with structural geology information, to interpret and understand the structural geometry a hazardous rockslide area may have and to construct a geological model of the site. Similarly, Ghiglieri et al. (2016) built a 3D hydrogeological-depositional model based on sequential stratigraphy and vertical electrical soundings (VESs). Thus, geophysical methods can provide useful data for decision-making in the early understanding of small-scale mineral deposits.

Zhang and Zhu (2018) discuss the role of three-dimensional geological modeling to build mining plans and to identify potential hazards during operation. As shown in the literature, three-dimensional geological models are commonly used for representing mineral deposits.

* Corresponding author.
E-mail address: ranyere.eng@gmail.com (R.S. Silva).

https://doi.org/10.1016/j.jappgeo.2022.104775
Received 15 July 2021; Received in revised form 26 May 2022; Accepted 3 August 2022
Available online 6 August 2022

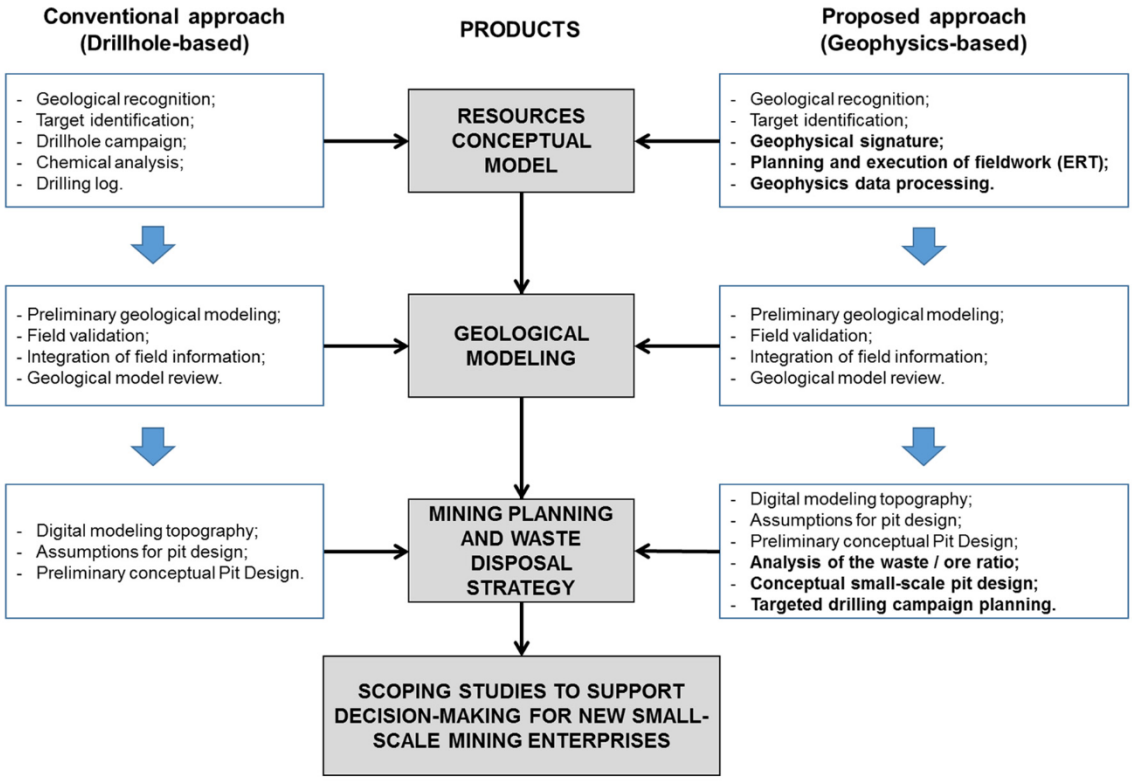

Fig. 1. Research methodology for project conceptual phase in small-scale mining.

These models are then employed to guide the different horizons of mining planning. Adeli et al. (2018) argue that three-dimensional geological models are an essential input for mineral resources evaluation and mine planning and, as such, it affects all subsequent stages of the mining process.

One critical aspect of long-term mining planning, including early-stage scoping studies, is the definition of the pit limits and the associated amount of waste that will be generated during the lifetime of a mine (ultimate pit limits problem). For this reason, the mining waste disposal strategy is a significant step in mining projects, in particular for small-scale mining. Ghose (2003) explains that small-scale mining has been the subject of intensive international debate, due to the need to promote cost-effective and sustainable development-oriented practices. According to Thornton (2014) the environmental aspect of small-scale mining sites is considered in a limited fashion, when compared to large-scale mining.

The present study proposes a cost-effective methodology to address the ultimate pit limits problem in small-scale mining, with an appropriate waste disposal strategy. The methodology employs data generated from Electrical Resistivity (ER) and Induced Polarization (IP) field tests to carry out the geological modeling of a small-scale deposit of barite. The resulting geological model was employed in the design of a conceptual pit and a waste disposal strategy that governed the economic model of the new enterprise, including the planning of a targeted drilling campaign.

2. Methodology

The methodology employed in the present study is a new approach for carrying out a conceptual pit design of small-scale deposit of barite. This method has combined aspects of applied geophysics, geological concepts and mineral engineering. First, two geo-electrical methods, ER and IP were used to determine thickness of barite bodies. Then, the geological model was built using the results of the two geophysics methods, after processing and analysis of these results. The ultimate pit design was carried out over the geological model, a digital topographic model, and other technical assumptions. Finally, a targeted drilling campaign was designed to generate new geological information in order to complement the future knowledge of the mineral resource assessment. Fig. 1 illustrates the methodology applied, and its comparison with more traditional methods.

2.1. Resources conceptual model

2.1.1. Geological recognition and target identification

The area to be studied is located on the Perau Formation, belonging to the Setuva Group (Silva et al., 1999), as shown in Fig. 2A. These authors characterize it by the presence of quartzitic and schistous units with metamorphism in the schist-green facies zone of the sericite, with occurrences of Pb-Zn-Ag (Cu—Ba), as shown in Silva et al. (1999) and Silva et al. (2019). The quartzite unit is composed of fine to medium-grained quartzites, with intercalations of micaceous, feldspar, conglomeratic levels and, locally, dolomitic or calcitic marbles and carbonate schist. The schist unit is of greater expression and is characterized by quartz-biotite schist and graphite-mica schist, locally with garnet and staurolite. In this unit there are amphibolite lenses and carbonate rock lenses (Silva et al., 2019). As defined by Campanha and Sadowski (1999), the depositional environment of the Perau Formation corresponds to an ocean floor volcanic sedimentary sequence, with the generation of a SEDEX deposit, which was subsequently subjected to metamorphism.

Field activities began with geological fieldwork near the barite outcrops, which has identified the following units: phyllite, marble, quartzite, schist, and barite. Fig. 2 shows the geological map of the properties, where the red polygons are the outcrops of barite.

In the study area, as described by Silva et al. (1999), the deposit is stratiform, with singenetic barite mineralizations that agree with the of the host rock bedding. The barite zone is interbedded with quartzites,

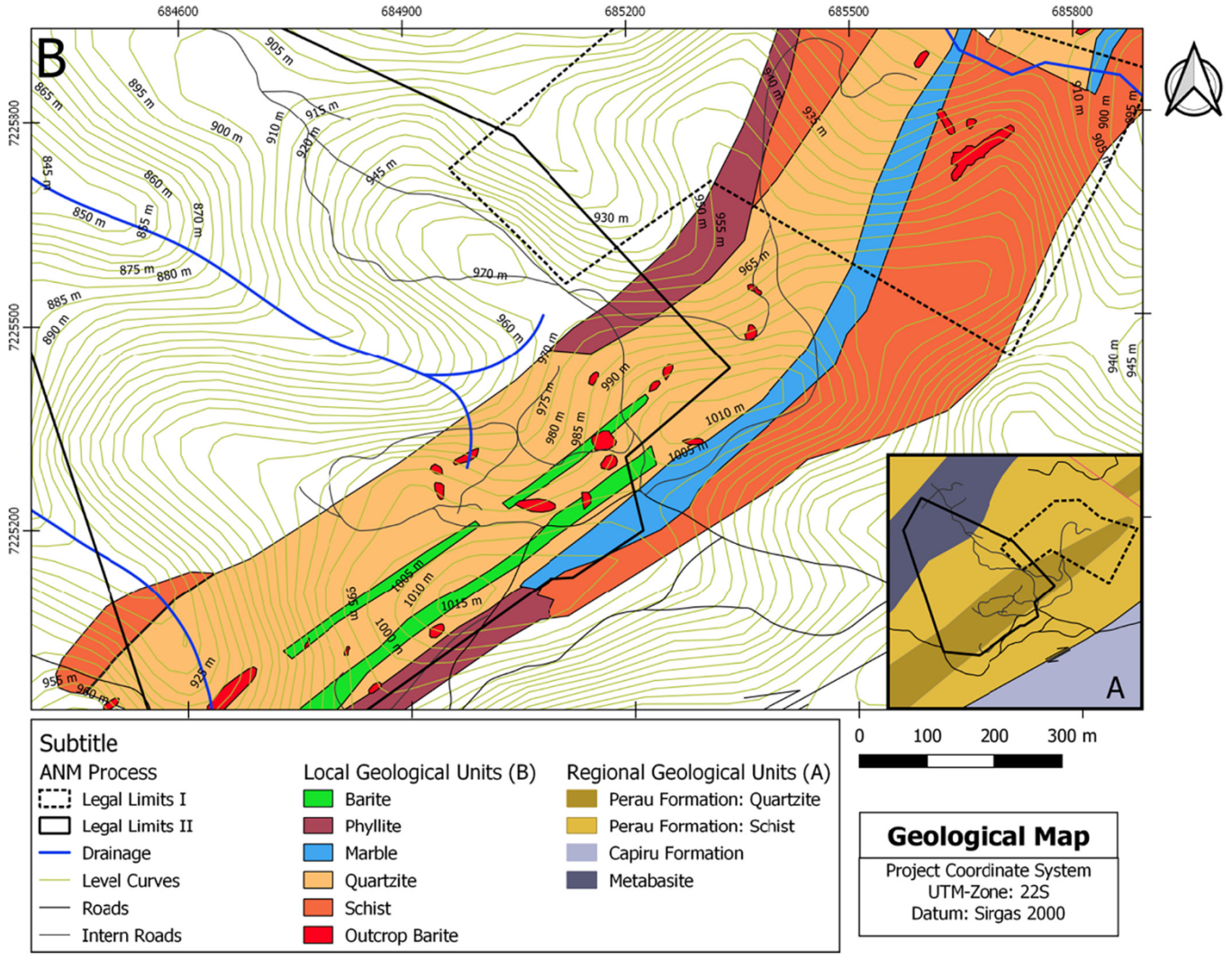

Fig. 2. Geological Map with Local and Regional Units. A: Geological Map with Regional Units. B: Geological Map with Local Units.

schist and metachert of Perau Formation. The main body of the deposit, hosted by schist and quartzites, is in the stratigraphic sequence approximately 50 m above the occurrences of Cu-Pb-Zn. The dip of the barite layer is N10E / 20NW in agreement with the sedimentary bedding. Thus, as the mineralized bodies have a low dip, the survey profiles were located along the outcrops or close to them.

In the first stage, the study area was mapped for geological fieldwork and target identification for geophysical signature. Then, geophysical activities were performed, so that it was possible to verify the geophysical signature of the barite deposits.

2.1.2. Barite Geophysics Signature

Due to the high density of barite (4.48 g/cm3) in relation to the other silicates (quartz 2.65 g/cm3, clay 2.60 g/cm3), gravimetry was considered at first, but due to the small thickness of the Barite occurrences in the region of interest, it was considered that the resolution of the method would not be appropriate. Bhattacharya et al. (1974) found that resistivity tests showed that barite bodies within gneisses, granites and basic rocks are more resistive and enable detection of barite veins, whereas gravimetric tests have failed.

This preliminary study to verify the geophysical signature was performed on two target lines, according Fig. 3.

The first target was a well-defined barite outcrop. The host rock of the outcrop was quartzite. An initial line was surveyed with a dipole-dipole array with 2 m of electrodes spacing. According to the field observations, the barite veins occurred at a distance of 14 m from the survey profile, with a thickness of about 1 m in the outcropping portion. The results of the test are presented in Fig. 4, where it is possible to observe a high resistivity zone between 9 and 28 m (dotted contour). This indicates the resistive zone associated to the barite occurrence.

The second target was a site with a possible barite occurrence. On this location, a survey with a 10-m spacing was carried out in order to locate highly resistive zones that could indicate the presence of barite. The profile obtained, illustrated in Fig. 5, shows two zones of interest: one in the central profile zone, between 80 and 90 m, and another highly resistive zone at the profile's end. This zone at the profile's end presents resistivity values similar to those of the barite zone in the first target investigated. This similarity indicates that this zone is the most suitable place for the continuation of the indirect prospecting surveys and, later, with direct investigation methods (drilling campaign). The relatively lower resistivity of the host rock is compatible with schists that occur in this profile, according to observations made during the geological fieldwork. There is no clear relation observed between chargeability and the barite body. High chargeability values could be related to the presence of sulfides (galena, pyrite, chalcopyrite) associated with the SEDEX deposit.

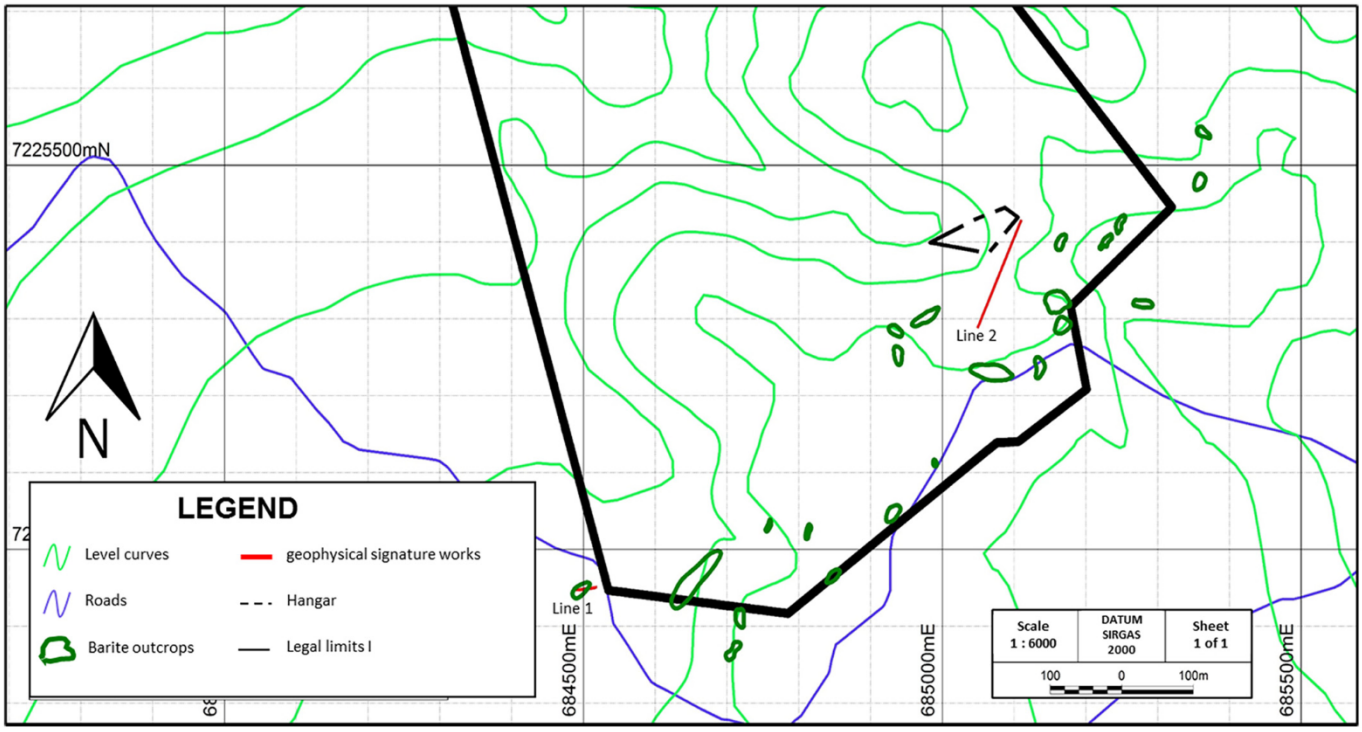

Fig. 3. Geophysical signature works.

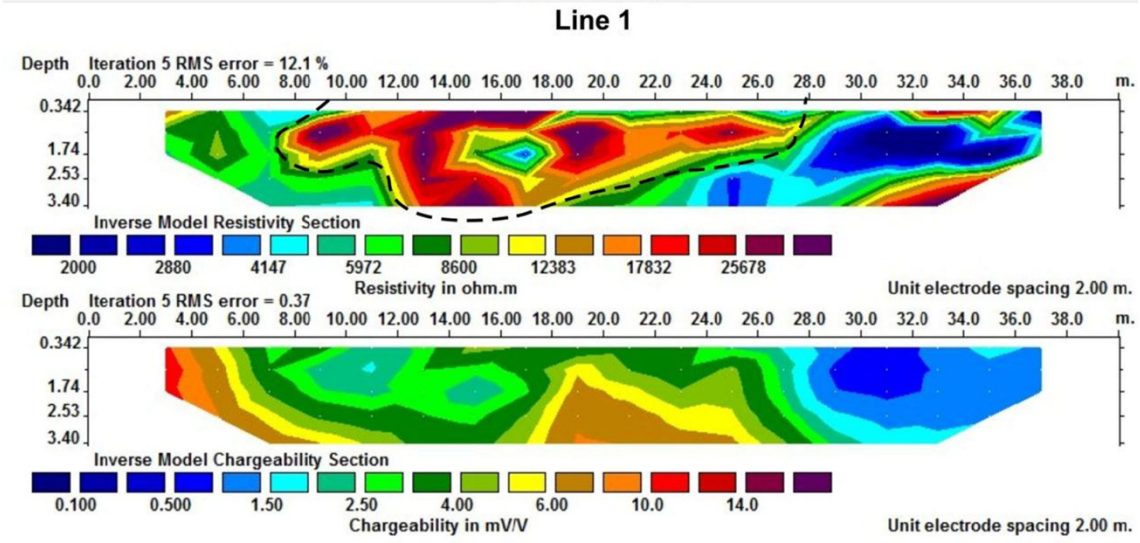

Fig. 4. Results of the electrical profile in Line 1 (dipole-dipole arrangement 2 m spacing).

2.1.3. Planning and execution of fieldwork

Initially, the survey targets were identified according to the outcrops of barite. After that, the geophysical surveys were planned and executed. The geophysical survey was planned out in locations with known outcrops, named as A, B, C, D, E, ET, G and J, as shown in Fig. 12. As the mineralized bodies have a low dip, the survey profiles were located along the outcrops or close to them. However, during the geological field work, it was observed that some minor bodies occur in the form of veins with a high dipping angle. This has indicated that sub-vertical anomalies related to the barite can occur in the results of the geophysical surveys.

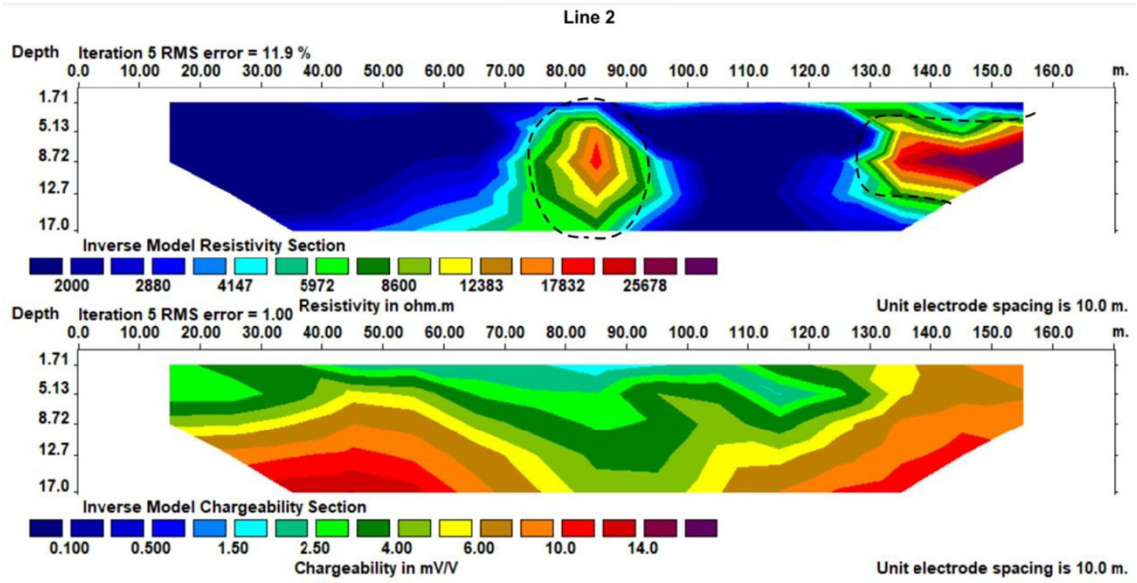

Fig. 5. Results of the electrical profile in Line 2 (dipole-dipole arrangement with 10 m spacing).
The black dotted contours in the center of the profile and at the end of the profile represent the resistive body (above 6000 Ω.m), which indicates the possible occurrence of barite.

The resistivity method is widely used due to its application in several research fields, i.e. mining, engineering, geology, hydrogeology and environmental. IP surveys are comparatively more common in mineral exploration studies.

Resistivity and IP surveys are carried out together, and although the IP method is somewhat more complex due to the interpretation demands, in many cases it can reduce ambiguity in the geophysical interpretation. In this case, the IP was applied to assess the possibility that the host rocks (schists and quartzites) presented a different IP response from barite.

Binley and Kemna (2005) explain that in the electrical resistivity method, the spatial variation of the resistivity ρ (or σ, its inverse conductivity) in the field is determined using four electrode measurements. Two electrodes are used to create an electrical circuit. The measurement of potential difference between the two other electrodes allows the calculation of the apparent resistivity (ie, the resistivity that a homogeneous space medium must have to provide the actual measurement). Electrodes are placed on the ground surface.

The calculation of the apparent resistivity that is given by:

$$\rho_a = K\frac{\Delta V}{I} \tag{1}$$

where: ρ_a = electrical resistivity (ohm.m), K = geometric factor, ΔV = potential difference and I = intensity of current.

Thus, it is possible to identify the different layers of soil, weathered rock and bedrock by means of the resistivity values obtained in field surveys. The true resistivity is calculated through an appropriate computational process. The relationship between the apparent resistivity and the true resistivity is quite complex. Apparent resistivity data is inverted to generate an interpreted resistivity model. The inversion process seeks to find a model that gives a response that is similar to the actual measured values (Geotomo Software, 2007). The resistivity model is an idealized mathematical representation of a section of the earth.

Several electrode configurations can be used for surface surveys. Dahlin and Loke (1997) evaluated several electrode arrays and their advantages and limitations, considering noise sensitivity and anomaly effects. The authors concluded that the anomaly effects for different arrays vary with local geology, and recommended the pole-dipole, dipole-dipole and Schlumberger arrays for 2D surveys. According to Loke (2002) the dipole-dipole array is the most sensitive for three-dimensional assessments, compared to the other arrangements most frequently used. This was the array chosen for the investigation of barite bodies.

The induced polarization (IP) method is based on the measurement of voltage variations as a function of time or frequency (Binley and Kemna, 2005). The present research employed IP measurement in the time domain. In time domain IP, using a standard four-electrode resistivity spread in a DC mode, if the current is abruptly switched off, the voltage between the potential electrodes does not drop to zero immediately. After a substantial initial decrease, the voltage suffers a gradual decay and can take many seconds to reach a zero value. The voltage decay is recorded during a time interval ⊗t = t2 - t1 (milliseconds) after the current flow is interrupted. The calculated parameter is the apparent chargeability Ma, given by:

$$M_a = \frac{1}{V_P}\int_{t_1}^{t_2} V(t)dt \tag{2}$$

where *V(t)* is the residual voltage at time t after the current interruption (mV), *Vp* is the primary voltage recorded during the current flow (V). M_a is in milliseconds or mV/V.

The amplitude of the residual voltage value is directly linked to the greater or lesser capacity that the geological materials have to polarize,

Table 1
Acquisition parameters.

Line	Distance between lines (m)	Profile length (m)	Acquisition parameters					RMS initial	RMS final	Iteration	Inversion parameters	
			Total number of data point	Number of electrodes	Number of data levels	IP*					Inversion methods	Flatness filter ratio
						Integration time (s)	Delay time (ms)					
A1		48	48	13	7	2	200	20.25	4.1	5	Smoothing constraint	1
A2	10	48	49	13	7	2	200	10.32	2.9	5	Smoothing constraint	1
A3		48	49	13	7	2	200	8.33	4.6	5	Smoothing constraint	1
B1		80	104	21	7	2	200	14.57	6.1	5	Smoothing constraint	1
B2	10	80	98	20	7	2	200	39.83	26.8	4	Smoothing constraint	1
B3		80	98	20	7	2	200	29.89	9.3	4	Smoothing constraint	1
C1		48	49	13	7	2	200	6.1	2.5	5	Smoothing constraint	1
C2	10	48	49	13	7	2	200	6.59	2.4	5	Smoothing constraint	1
C3		40	35	11	7	2	200	7.1	2.8	5	Smoothing constraint	1
D1	10	36	28	10	7	2	200	19.48	7.5	4	Smoothing constraint	1
D2		36	28	10	7	2	200	14.59	4.7	5	Smoothing constraint	1
E1		44	41	12	7	2	200	13.65	3.8	5	Smoothing constraint	1
E2	10	40	35	11	7	2	200	24.33	4.7	5	Smoothing constraint	1
E3		52	56	14	7	2	200	19.6	11.9	3	Smoothing constraint	1
ET1	10	60	70	16	7	2	200	22.41	11.7	4	Smoothing constraint	1
ET2		64	77	17	7	2	200	14.58	8.1	5	Smoothing constraint	1
G3	–	44	42	12	7	2	200	12.47	4.6	5	Smoothing constraint	1
J1		48	49	13	7	2	200	16.2	4.3	5	Smoothing constraint	1
J2	10	48	49	13	7	2	200	15.18	5.8	5	Smoothing constraint	1
J3		48	49	13	7	2	200	15.76	10.3	5	Smoothing constraint	1

thus constituting the basis of the method. This polarization capability constitutes the IP susceptibility of earth materials. Distinct mechanisms can generate the polarization response of the media.

The IP phenomena is observed when metallic bodies and metallic dispersed particles are present in the subsurface, resulting from differences in ionic mobility in the metallic particles and ions in the pore fluid (electrode polarization). Another source of polarization are ion selective zones formed by clay particles and/or pore throats (membrane polarization). Charge motion along the electrical double layer (EDL) formed at the mineral surface also contributes to polarization (electrochemical polarization).

Resistivity and IP surveys are carried out together, hence data acquisition is carried out with the same electrode array. As it is the case for resistivity, true chargeability is calculated through appropriate computational processes.

The application of the electrical resistivity and induced polarization methods was carried out using the electrical profiling technique.

Electrical profiling provides a more realistic 2D analysis, where the resistivity and IP values are continuously investigated vertically and horizontally along the survey line, even in the presence of geological and topographical complexities. It has been used successfully as technique for investigating shallow subsurface electrical structures in various environments, such as earthquake-associated faults (Yang et al., 2002), permafrost (Hauck et al., 2003), substream sediments (Crook et al., 2008), and ore prospecting (Heritiana et al., 2019). The surveys are carried out along profiles and the results are presented in the form of 2D sections, where bodies and layers with different electrical properties can be identified for later geological interpretation.

In the present research, the geophysical survey was performed on oblique profile to the bodies, with the objective of verifying their continuity in depth and laterally. Observations were made in existing excavations in the area and it was verified that the bodies sometimes had a thickness of a few meters. Because of this, the chosen dipole-dipole array used electrode spacing of 4 m, with 7 investigation levels and cell width equal to the electrode spacing. A group of geophysical lines was positioned in each of the studied sections (A, B, C, D, E, ET, G and J). Table 1 presents the acquisition parameters used to carry out the surveys.

2.1.4. *Geophysics data processing*

After the geophysical surveys, it was possible to process the data obtained by the campaigns carried out at each target location. The data processing was performed in a specialized software of geophysical data interpretation.

The interpretation took into account site-specific resistivity and chargeability properties and parameters. This information fed the interpreting process of the distribution of barite bodies along the

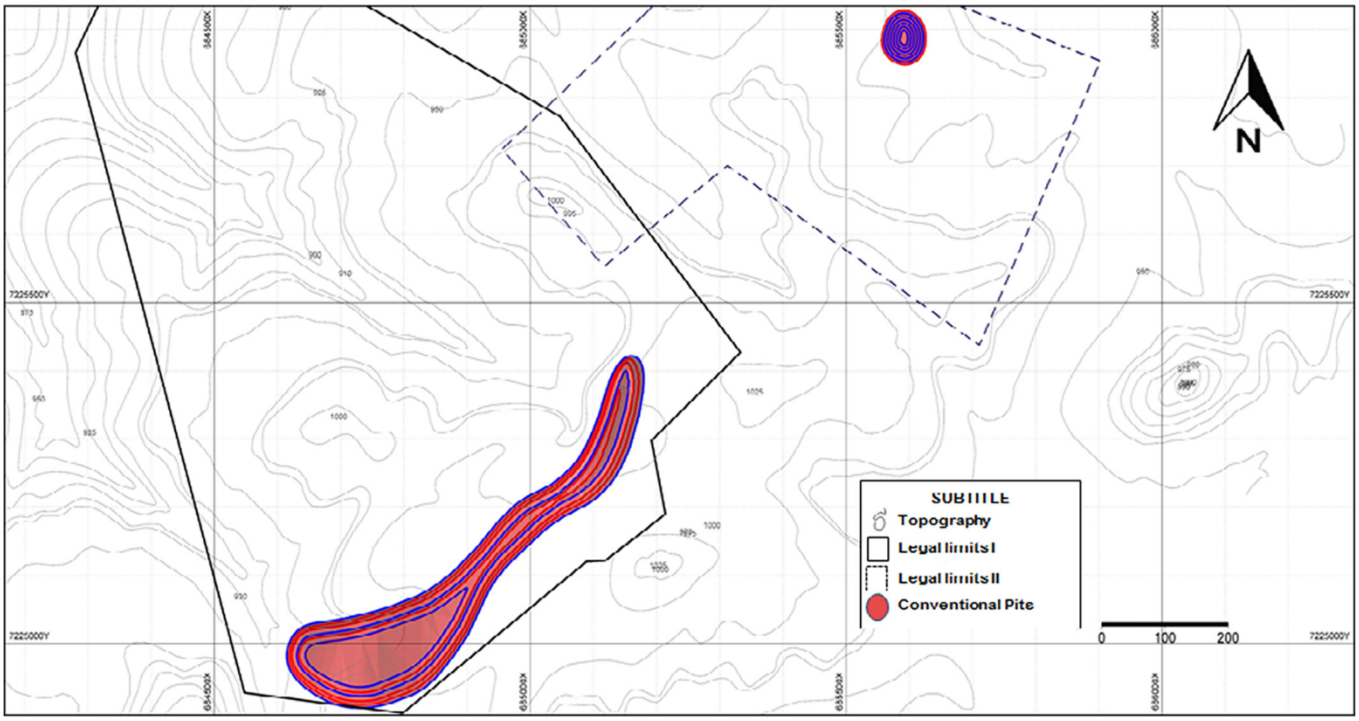

Fig. 6. Pit conceptual in the conventional approach.

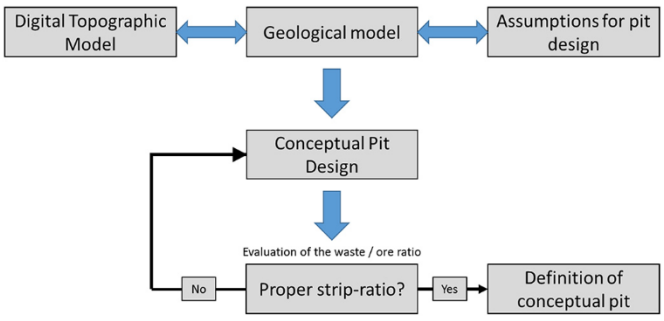

Fig. 7. Design procedure of the conceptual pits.

deposit.

2.2. Geological modeling

The geological interpretation resulted in the construction of a geological model composed of barite bodies for each one of the studied targets (A, B, C, D, E, ET, G, J). These ore bodies were converted into a geological block model, according to predefined grid of spatial dimensions.

The block model used data from parallel lines of ERT (Electrical Resistivity Tomography) with 10 m of distance between them. According to Dahlin and Loke (1997) the dipole-dipole array is the most sensitive to three-dimensional effects, compared to the other arrays most frequently used in ERT, providing lateral information up to a distance of 3 times the spacing between the electrodes. Thus, the parallel lines of ERT provided important information to evaluate the three-dimensional shape of the barite bodies.

The geological model of the barite ore body is based on the tracing of planar polygons (sections) that define the limits of the mineral body. The geological sections are built plane by plane, in which the tracing of each polygon is defined individually, according to a region of influence. That is, each control section represents an individual interpretation of the ore body information.

The generation of the three-dimensional model followed the same technique used by Martins et al. (2016a, 2016b), improving the level of information required to generate a geological model, reducing processing time and costs.

The geological model allowed a preliminary quantification of the potential resources in the area of study. After fieldwork, the geological model was validated with field observations. This information was integrated into the geological model, which was revised and used for the ultimate pit design. The geological model also allowed the planning of the targeted drilling campaign in the area of study. A conceptual pit analysis was also carried out for the barite bodies identified and modeled in the previous steps.

2.3. Mining planning and waste disposal strategy

Rahimi et al. (2018) explain the Ultimate Pit Limit (UPL) as the pit which, when compared with other potential pits, offers the highest net present value (NPV). The ultimate pit definition is essential for establishing the economic potential of a deposit, in order to estimate the ore mass and waste to be exploited, as well as the life of the mine, according to a given production rate. In small-scale mining, success of the enterprise is closely associated with the reduction of the geological uncertainties in the early stages of the project.

Meagher et al. (2014) discuss that open-pit mine design and long-term production planning are important steps in initiating mining ventures. The ultimate pit represents the maximum volume of economically viable material to be extracted (Campos et al., 2018). Samavati et al. (2018) emphasize the fact that the ultimate pit limits are defined once the costs associated with mining, mineral processing and waste disposal exceeds the revenues obtained from selling the processed material. Rahmanpour and Osanloo (2017) and Chatterjee et al. (2016) consider the ultimate pit limit determination a strategic decision, because it triggers the amount of mineral reserves, stripping ratio, location of waste dump and tailings dam, and the land use associated with the mining enterprise. Marcotte and Caron (2013) add that the definition of

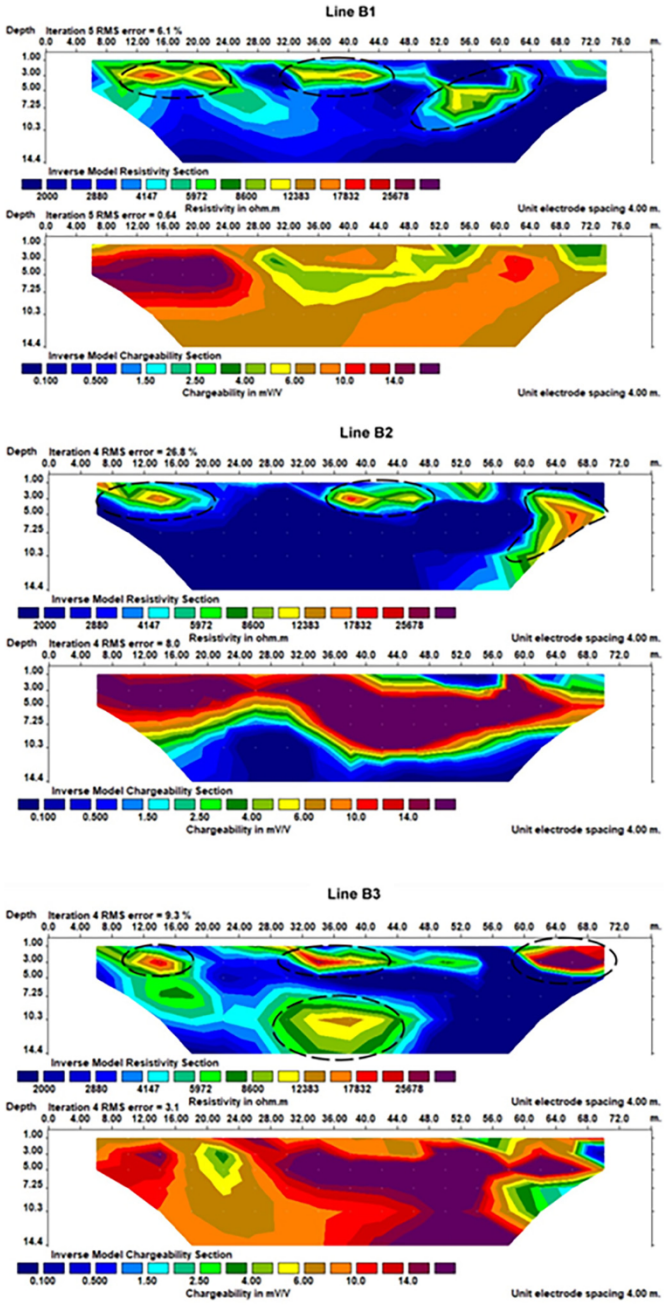

Fig. 8. Results from geophysical surveys - Section B (Lines B1, B2 and B3). The reading lines in section B reveal the existence of several bodies with high resistivity near the surface (3 bodies) and a deeper body that occurs in Line B3.

ultimate pit limits is a critical aspect in pre-feasibility and feasibility studies of mining enterprises. In addition, it is the basis for important initial decisions on open pit mining projects, such as production capacity, choice of equipment, and location and size of surface installations.

A conceptual pit was designed so that it would comprise most of the geological blocks generated. However, this conventional approach resulted in a pit with a very high stripping ratio, with a significant amount of waste to be removed (Fig. 6), compared to the quantity of barite ore that would be extracted.

This high volume of waste removal is explained by the form of occurrence of barite bodies in pooled pockets. Thus, it was decided to design several small-scale conceptual pits, one for each grouping of barite pockets, as shown in Fig. 14.

The procedure adopted for the design of the conceptual pit was divided into two stages, as shown in Fig. 7. The first stage started with the topographic model and the geological model, over which the initial conceptual pits were defined according to the established assumptions. The second stage consisted of the evaluation of the stripping ratio for each new pit, and the adjustment of the configuration of the conceptual pits in order to reduce the stripping ratio for each individual pit.

The choice of geometric parameters is an important step for mining planning as it takes into account issues related to the geological deposit, operational safety and mine productivity as well as the most appropriate definition of the waste disposal strategy.

According to Alegre et al. (2019), geotechnical parameters (face angle, bench width and height) affect the overall angle of the final pit, as well as the waste and ore mass, and consequently the stripping ratio (waste/ore). Fredj et al. (2020) report that failure to comply with geotechnical parameters in most cases can lead to critical situations and disastrous mining results.

The slope angle is directly related to the geotechnical parameters (orientation and discontinuity resistance) of the mining area and is therefore a constraint on the definition of the pit geometry (Altuntov and Erkayaoğlu, 2021).

Moses et al. (2020) used 45° as the general slope angle of a conceptual open pit mine design. This general slope angle was conservatively chosen to maximize the safety of the general slope, avoiding slope instability. Thus, the general slope angle of 45° used in the conceptual model took into account the absolute angle of repose of the materials and the general slope stability.

The pit design assumptions adopted for the pit design in the present research were as follows:

- Overall slope angle: 45°;
- Bench height: 5 m;
- Width of the berm: 4 m.

These parameters were applied to the design of each conceptual pit in order to evaluate and adjust the stripping ratio as required.

3. Site description and data collection

The study area is located in the Vale do Ribeira Region, State of Paraná, Brazil. This region is inserted in the geotectonic context of the Mantiqueira Province. It includes, in addition to the Ribeira Orogen (where the area is located), the orogens of Araçuaí, Southern Brasília, Dom Feliciano and São Gabriel. This province, as defined by Almeida (1977) includes the south and southeast coastal regions, forming a NE-SW belt bordered by the provinces of Tocantins, São Francisco and Paraná, and the east side is bound by the continental margin and coastal basins of Espírito Santo, Campos, Santos and Pelotas.

According to Vieira et al. (2018), there following domains are present in the Ribeira Belt: Varginha, Embu, Costeiro, São Roque, Apiaí, Curitiba, Paranguá, and Luís Alves. The study area is in the Apiaí Domain, which together with the Curitiba and Luis Alves domains, make up the southern part of the Belt. The Apiaí domain comprises terrain compounds formed during the Pan African Brazilian Orogeny and it includes backarc basin assemblies, carbonate platform deposits, turbidites, and deep water assemblies associated with mafic magmatism (Faleiros et al., 2014). The basement rocks present in this domain outcrop mainly in the nucleus of antiform structures, characterized as an association of migmatitic-mylonitic orthogneisses and have robust geological complexity (Faleiros, 2008).

Data-collection employed a Syscal Pro equipment (Iris Instruments), a resistivity-meter that records resistivity and chargeability measurements. Metallic electrodes were used for current injection and non-polarizing electrodes (Cu/CuSO4) were used for potential measurement. Data were collected with separated cables for current transmission and potential measurement. Current was injected in 2-s cycles. IP

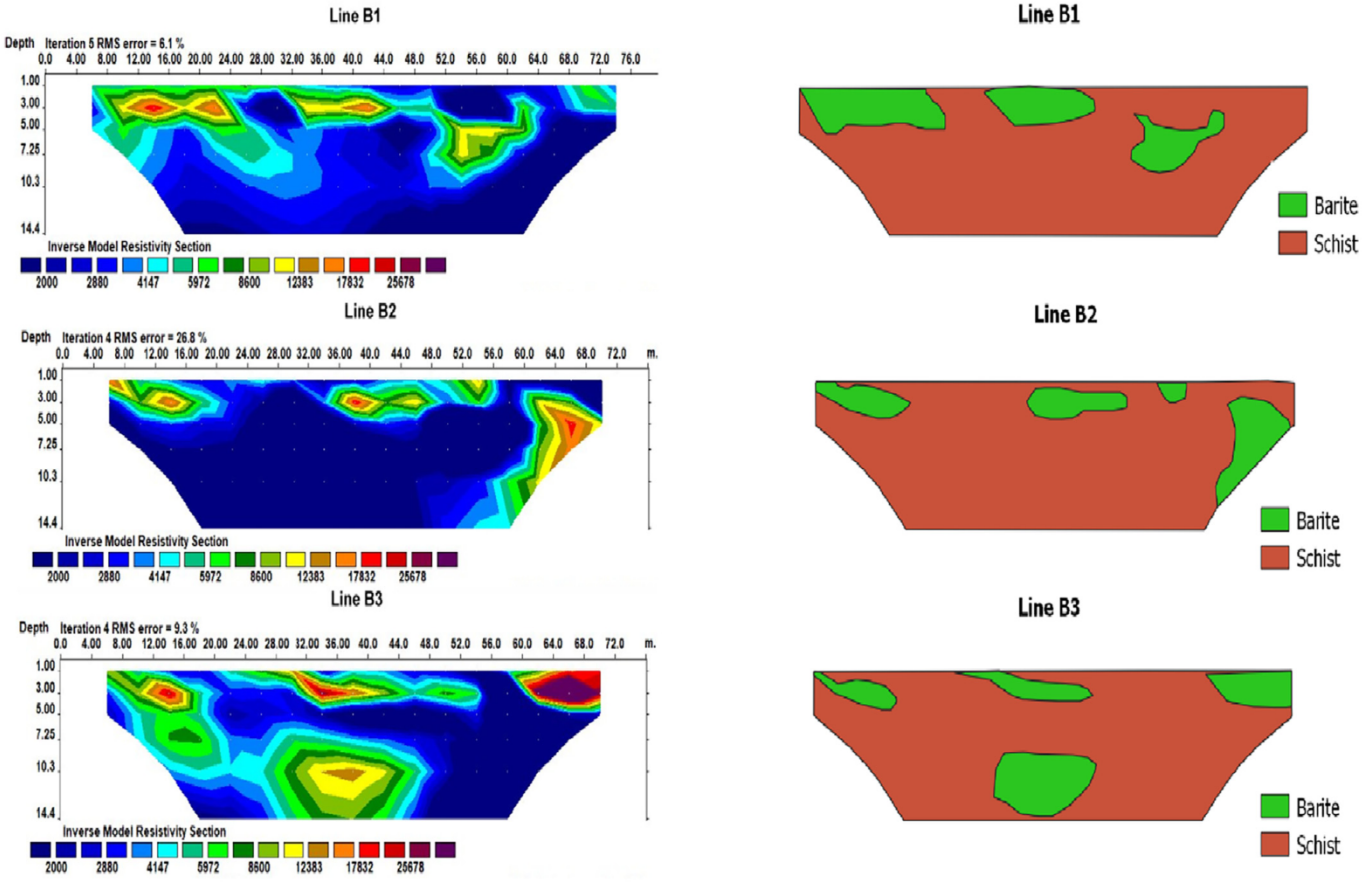

Fig. 9. Results of the 2D interpretation of the integration to three lines (B1, B2 and B3).

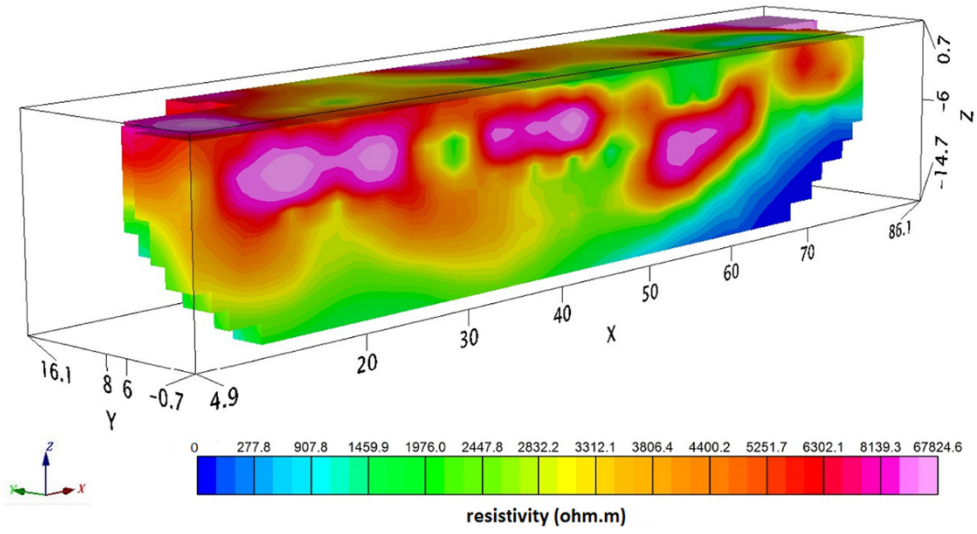

Fig. 10. Results of the 3D interpretation (Lines B1, B2 and B3).

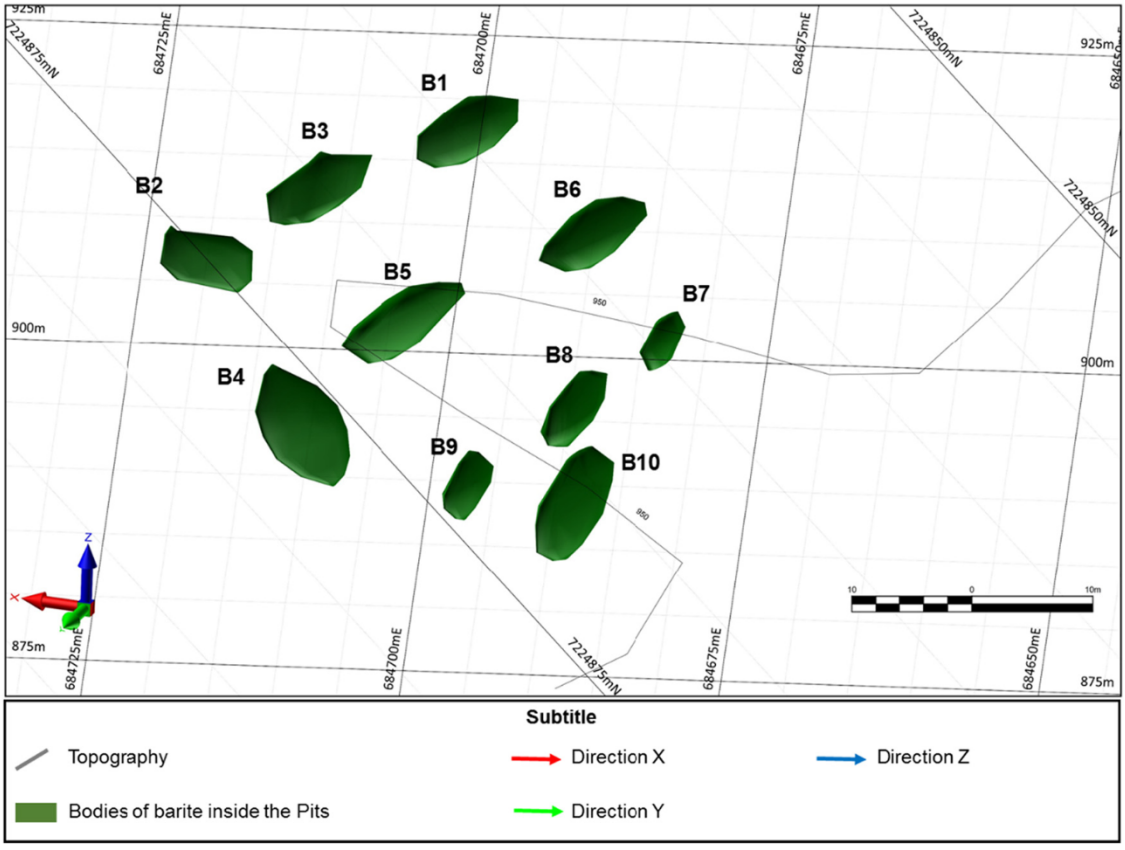

Fig. 11. Three-dimensional view of the geological model of section B, highlighting the bodies from B1 to B10.

measurements were recorded after a 200 milliseconds delay from the current shut off. The data were interpreted using the least-square method with smoothing constraint inversion routine using the commercial software RES2DINV (Geotomo Software, 2007).

4. Processing and Inversion of geoelectrical data

The profiles were positioned in the outcrops of barite. In each outcrop, three profiles were surveyed, the first on the outcrop and the other parallel and positioned in the direction of the dip of the body to delimit its geometry in the subsurface. For all profiles, the same color scale and 4-m spacing between the electrodes were used.

The field surveys produced 8 geophysical sections (A, B, C, D, E, ET, G, J). Fig. 7 shows the results of the profiles investigated in section B. In this body, three profiles (B1, B2 and B3 of lengths 80, 76 and 76 m) were positioned.

The resistivity sections show that the high resistive zones (> 8000 Ω.m) closest to the surface (up to 5 m deep) are related to the presence of barite observed in the outcrop in Line B1. The host rocks observed in the outcrop are quartzites, and have lower resistivity values than barite (<4000 Ω.m).

It is not possible to make a direct correlation of the most resistive zones with chargeability, which indicates that the barite bodies are not polarizable. The host rock below the barite bodies tends to have slightly higher chargeability values (6 to 15 mV / V), which is possibly related to a small amount of sulfides.

Fig. 10 shows a 3D view of the model resulting from the integration of the three profiles showing the the bodied with resistivities >8000 Ω.m. The fragmentation of the high resistive zones indicates that the barite body is not continuous. The fragmentation of the resistive body shows resistive zones in positions of 20 m, 40 m, and between 50 and 60 m, always in the shallower portions of the deposit. The fragmentation of the high resistive zones indicates that the barite body is not continuous, with several small bodies with high resistivity.

The reading lines in section B reveal the existence of several bodies with high resistivity, less than a dozen meters apart, that occur near the surface (3 bodies) and a deeper body that occurs in Line B3.

The induced polarization data do not differentiate barite bodies. Although IP did not show good results, it was considered important to keep the results in the article so that other researchers can use this information in their research.

5. Geological modeling and interpretation

Fieldwork results indicated that areas with barite are associated with high resistivity values, usually above 8000 Ω.m, as shown in Fig. 8.

The results obtained in the resistivity tests indicate potential occurrences of barite in all profiles. However, there are more promising anomalies, with possible larger bodies. Fig. 9 presents the results of the 2D interpretation for section B, based on the results obtained with ERT.

The results of the surveys carried out in sections A, C, D, E, ET, G, J and their respective 2D interpretations are shown in Figs. S1, S2, S3, S4, S5, S6 and S7, contained in the supplementary material file.

The 3D interpretation (Fig. 10) and preliminary geological modeling (Fig. 11) provides an indication of the preliminary values for the volumes and masses of barite in the bodies identified in the geophysical survey. The modeled spheroids are based on the circles dotted of the 2D profiles.

The results of the 3D interpretation carried out for sections A, C, D, E, ET, J are shown in Figs. S8, S9, S10, S11 and S12, contained in the supplementary material file.

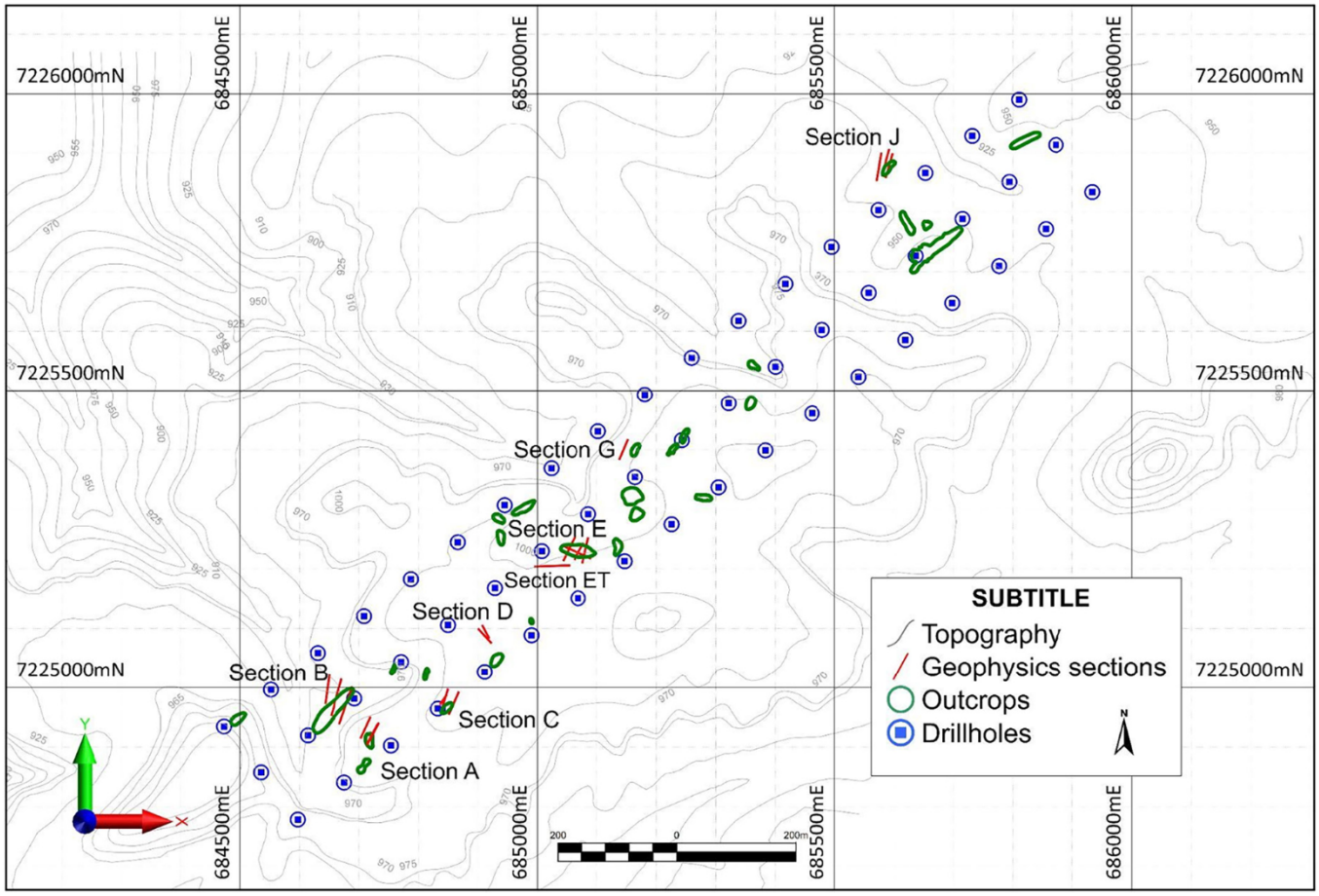

Fig. 12. Conventional approach for drilling campaign (Drillhole-based).

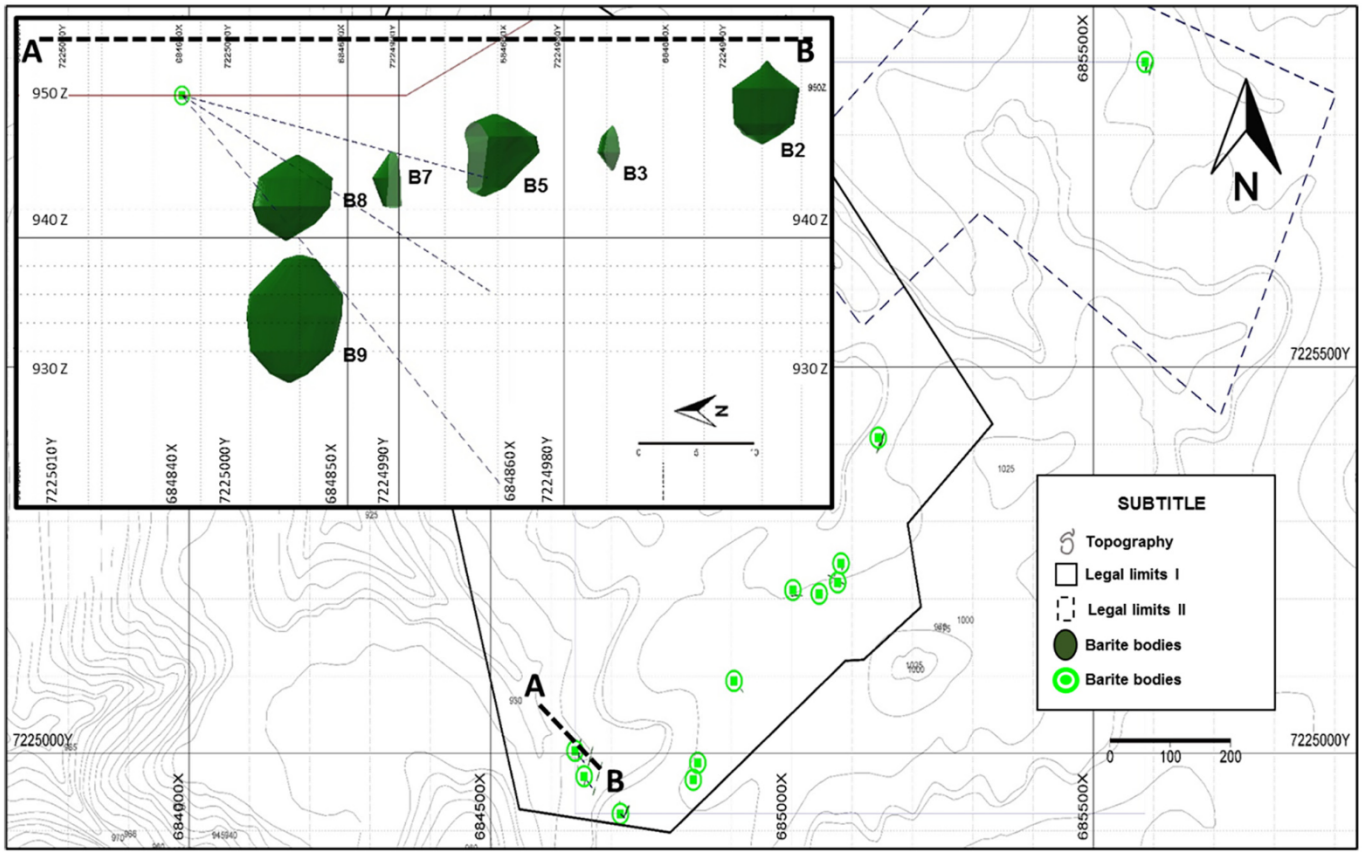

Fig. 13. Proposed approach for targeted drilling campaign (Geophysics-based).

6. Results and discussion

The results of the preliminary geological modeling process also allowed for the planning of a targeted drilling campaign. Unlike the conventional approach (drillhole-based), the proposed approach (geophysics-based) reduced the drilling costs required to configure a potential mining enterprise. Fig. 12 presents the drilling plan using a conventional approach (drillhole-based).

The geological model built from the geophysical survey results allowed a targeted drilling campaign planning to confirm the location and orientation of the identified barite bodies as well as to validate the estimated thicknesses (Fig. 13).

Fig. 13 shows the spatial distribution of the drill holes of the target campaign and a detailed profile with the planned trajectory of a hole in Section B.

The targeted drilling campaign was designed to reduce geological uncertainties even before the start of the drilling campaign. This reduction may enable new investments for projects that are in the scoping study phase. In this research, the study of the conceptual pit quantified the potential mass of material to be mined, proving the preliminary economic viability of the barite deposit, which in turn justified the planning and expenditures of the targeted drilling campaign.

In the conventional approach, 54 holes with depth of 40 m each (Fig. 12) would result in 2160 m drilled. The new configuration reduced the total drilling to 688 m as shown in Fig. 13.

The results obtained by the geological model allowed the design of a series of small-scale pits. Only one of those pits resulted in a fairly high stripping ratio (Fig. 5) because it is associated with a larger barite body. Fig. 14 shows the pit design results and their distribution along the area, and Fig. 15 presents a detailed image of conceptual pit B.

The new pit design configuration reduced the waste disposal from over 1.7 million tonnes to nearly 130 thousand tonnes, a reduction of 92%.

For the cost reduction of the target drilling campaign, the reference price of the rotary survey per meter, according to the current practice in southern Brazil, is R$ 200.43 (DAER, 2016). The average drilling rate is 1.25 m per hour. The values considered for the targeted drilling campaign include costs of rotary drilling and the geophysical survey (according to the costs incurred in the field work).

Table 2 summarizes the savings with the proposed approach vs. the conventional one in relation to costs, work time and deposition waste.

7. Conclusions

The present study considered 3 innovative aspects to address small-scale mining issues of mineral deposits: use of resistivity in a small-scale barite deposit, targeted drilling campaign planning and reduction in the amount of waste disposal. The results of the study point towards the importance of employing geophysical signature tests before conducting investigative geophysical campaigns. The initial tests showed that, even with the high density of barite when compared to silicates, the resistivity method is more adequate than the gravimetry method due to the small thickness of the barite veins, making the resolution of the gravimetry method inefficient, confirming the existing literature. The geological modeling of the barite occurrences through the geophysical results allowed the estimation of the preliminary quantification of the amount of material present in the deposit. In addition, the interpretation of the geophysical profiles and the construction of the geological model allowed the planning of a targeted drilling campaign. The implementation of this campaign avoided the execution of unnecessary drill holes, even before the start of the drilling campaign. The conceptual pit design allowed the estimation of the mass of material to be mined, proving the preliminary economic viability of the barite deposit, justifying the planning and expenditures of the targeted drilling campaign.

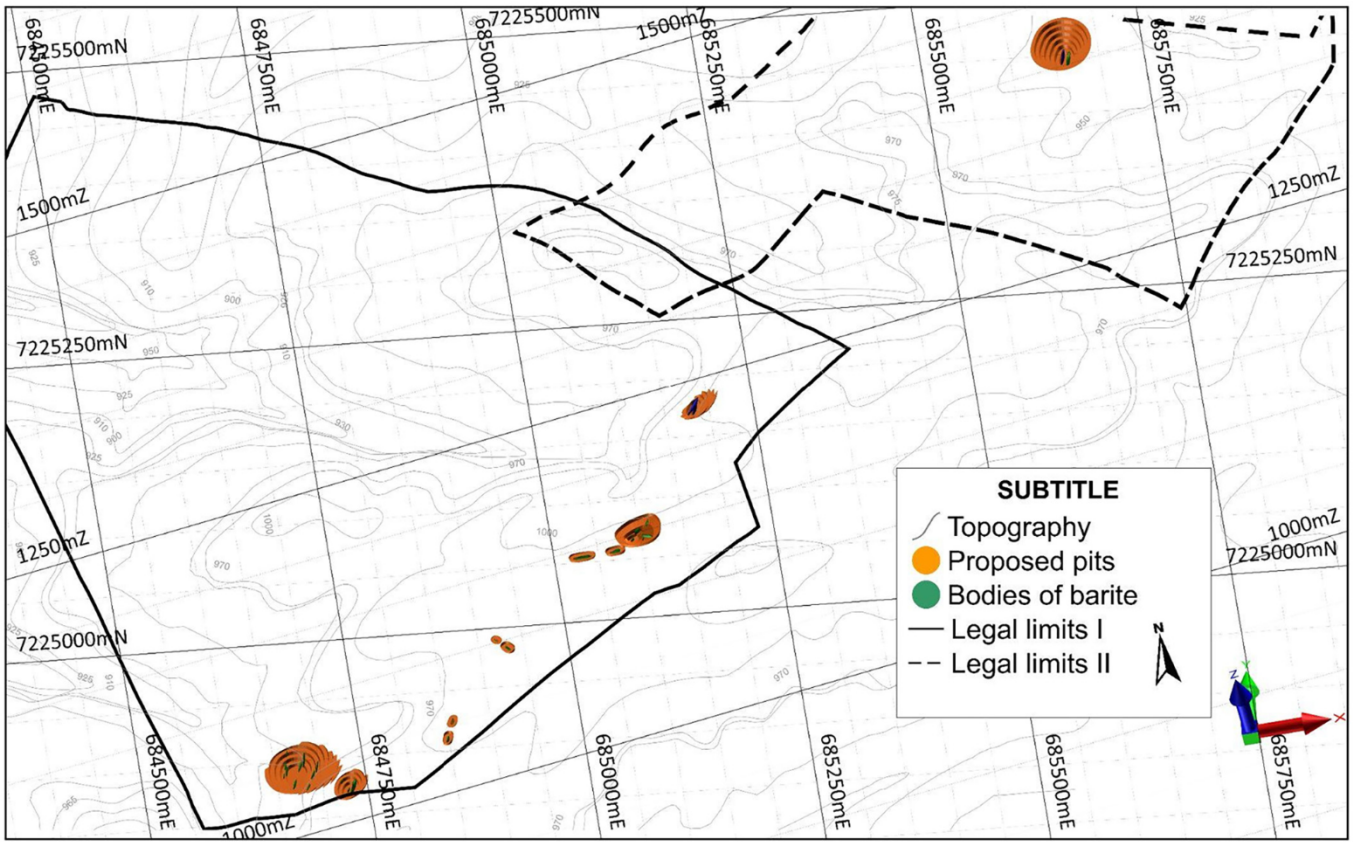

Fig. 14. Conceptual pits for the barite deposit modeled by geophysical methods (Proposed approach).

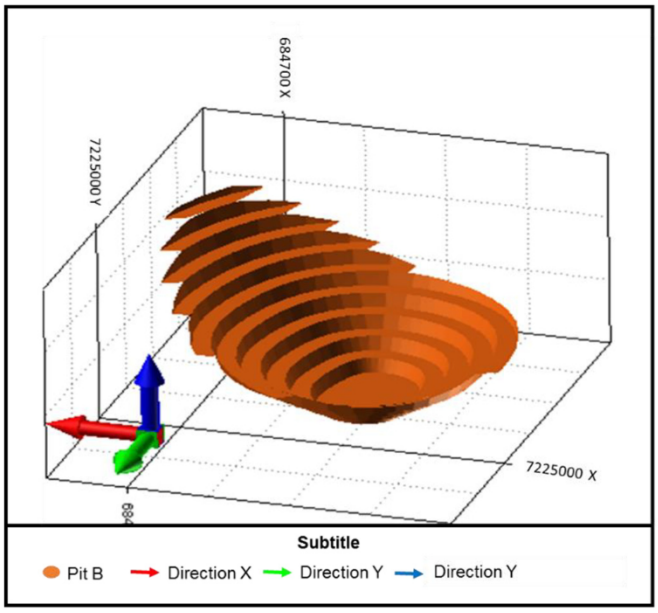

Fig. 15. Highlight for conceptual pit B.

These innovative aspects, applied in the project's conceptual phase, can contribute towards making small-scale mining more competitive. The targeted drilling campaign provided savings of over 58% with the reduction of nearly 62% in work time. The conceptual small-scale pit design resulted in a reduction of nearly 93% in generated waste against conventional approaches.

Table 2
Main obtained gains with the proposed approach.

Approach	Geological research (US$)	Time (Days)	Deposited waste (t)
Conventional approach	432,929	113	1,733,348
Proposed approach	179,896	43	127,069
Savings	58.45%	61.78%	92.67%

Declaration of Competing Interest

RANYERE SOUSA SILVA reports financial support was provided by Coordenação de Aperfeiçoamento de Pessoal de Nível Superior (CAPES - Brazil). GIORGIO DE TOMI, VAGNER ROBERTO ELIS reports a relationship with University of Sao Paulo that includes: employment.

Acknowledgements

The authors acknowledge support from the Coordenação de Aperfeiçoamento de Pessoal de Nível Superior (CAPES - Brazil). The authors also thank Micromine for providing the mining specialized software.

Appendix A. Supplementary data

Supplementary data to this article can be found online at https://doi.org/10.1016/j.jappgeo.2022.104775.

References

Adeli, A., Emery, X., Dowd, P., 2018. Geological Modelling and Validation of Geological Interpretations via simulation and Classification of Quantitative Covariates. Minerals. 8, 7. https://doi.org/10.3390/min8010007.

Alegre, D.A.G., Peroni, R.L., Aquino, E.R., 2019. The impact of haulroad geometric parameters on open pit mine strip ratio. REM, Int. Eng. J. [online]. 72, 25–31. https://doi.org/10.1590/0370-44672018720136.

Almeida, F.F.M., 1977. O Craton do São Francisco. Revista Brasileira de Geociências 7, 349–364. https://doi.org/10.5327/rbg.v7i4.128.

Altuntov, F.K., Erkayaoğlu, M., 2021. A New Approach to Optimize Ultimate Geometry of Open Pit Mines with Variable Overall Slope Angles. Nat. Resour. Res. 30, 4047–4062. https://doi.org/10.1007/s11053-021-09911-8.

Bhattacharya, B.B., Jain, S.C., Mallick, K., 1974. Geophysical Prospecting for Barite*. Geophys. Prospect. 22, 421–429. https://doi.org/10.1111/j.1365-2478.1974.tb00096.x.

Binley, A., Kemna, A., 2005. DC Resistivity and Induced Polarization Methods. In: Hydrogeophysics. Springer, Netherlands, Dordrecht, pp. 129–156. https://doi.org/10.1007/1-4020-3102-5_5.

Campanha, G.D.C., Sadowski, G.R., 1999. Tectonics of the southern portion of the Ribeira Belt (Apiaí Domain). Precambrian Res. 98 (1–2), 31–51. https://doi.org/10.1016/S0301-9268(99)00027-3.

Campos, P.H.A., Cabral, I.E., Ortiz, C.E.A., Morales, N., 2018. Comparison between the application of the conventional mine planning and of the direct block scheduling on an open pit mine Project. REM - Int. Eng. J. 71, 269–274. https://doi.org/10.1590/0370-44672017710037.

Chatterjee, S., Sethi, M.R., Asad, M.W.A., 2016. Production phase and ultimate pit limit design under commodity price uncertainty. Eur. J. Oper. Res. 248, 658–667. https://doi.org/10.1016/j.ejor.2015.07.012.

Crook, N., Binley, A., Knight, R., Robinson, D.A., Zarnetske, J., Haggerty, R., 2008. Electrical resistivity imaging of the architecture of substream sediments. Water Resour. Res. 44 https://doi.org/10.1029/2008WR006968.

DAER (Brazilian Department of Public Highways), 2016. Table of Service Fees. See. http://www.daer.rs.gov.br/upload/arquivos/201608/02133624-4tabela-projeto-maio-16-oficial.pdf (accessed: 16 December, 2019).

Dahlin, T., Loke, M.H., 1997. Quasi-3D resistivity imaging: Mapping of 3D structures using two dimensional de resistivity techniques. In: 3rd Meeting Environmental and Engineering Geophysics, Aarthus, Denmark, pp. 143–146.

Faleiros, F.M., 2008. Evolução de terrenos tectono-metamórficos da Serrania do Ribeira e Planalto Alto Turvo (SP, PR). https://rigeo.cprm.gov.br/handle/doc/268.

Faleiros, A.M., Campanha, G.A., Faleiros, F.M., Bello, R.M., 2014. Fluid regimes, fault-valve behavior and formation of gold-quartz veins - the Morro do Ouro Mine, Ribeira Belt, Brazil. Ore Geol. Rev. 56, 442–456. https://doi.org/10.1016/j.oregeorev.2013.05.002.

Fredj, M., Hafsaoui, A., Riheb, H., Boukarm, R., Saadoun, A., 2020. Back-analysis study on slope instability in an open pit mine (Algeria). Natsional'nyi Hirnychyi Universytet. Naukovyi Visnyk. 24–29. https://doi.org/10.33271/nvngu/2020-2/024.

Ganerød, G.V., Grøneng, G., Rønning, J.S., Dalsegg, E., Elvebakk, H., Tønnesen, J.F., Kveldsvik, V., Eiken, T., Blikra, L.H., Braathen, A., 2008. Geological model of the Åknes rockslide, western Norway. Eng. Geol. 102, 1–18. https://doi.org/10.1016/J.ENGGEO.2008.01.018.

Geotomo Software, 2007. RES2DINV. Rapid 2D resistivity and IP inversion using the least-squares methods. User's Manual, p. 138.

Ghiglieri, G., Carletti, A., Da Pelo, S., Cocco, F., Funedda, A., Loi, A., Manta, F., Pittalis, D., 2016. Three-dimensional hydrogeological reconstruction based on geological depositional model: a case study from the coastal plain of Arborea (Sardinia, Italy). Eng. Geol. 207, 103–114. https://doi.org/10.1016/j.enggeo.2016.04.014.

Ghose, M., 2003. Indian small-scale mining with special emphasis on environmental management. J. Clean. Prod. 11, 159–165. https://doi.org/10.1016/S0959-6526(02)00035-5.

Hauck, C., Vonder Muhll, D., Maurer, H., 2003. Using DC resistivity tomography to detect and characterize mountain permafrost. Geophys. Prospect. 51, 273–284. https://doi.org/10.1046/j.1365-2478.2003.00375.x.

Heritiana A., R., Riva, R., Ralai, R., Boni, R., 2019. Evaluation of flake graphite ore using self-potential (SP), electrical resistivity tomography (ERT) and induced polarization (IP) methods in east coast of Madagascar. J. Appl. Geophys. 169, 134–141. https://doi.org/10.1016/j.jappgeo.2019.07.001.

Marcotte, D., Caron, J., 2013. Ultimate open pit stochastic optimization. Comput. Geosci. 51, 238–246. https://doi.org/10.1016/j.cageo.2012.08.008.

Martins, A.C., Elis, V., Tomi, G., Bettencourt, J., Marin, T., 2016a. Resistivity and induced polarization to support morphological modeling in limestone mining. Geofis. Int. 55, 227–238. https://doi.org/10.19155/geofint.2016.055.4.1.

Martins, A.C., Terenci, E.R., Tomi, G., Tichauer, R.M., 2016b. Impact of Geophysics in Small-Scale mining. J. Remote Sens. GIS 05 (04).

Meagher, C., Dimitrakopoulos, R., Avis, D., 2014. Optimized open pit mine design, pushbacks and the gap problem—a review. J. Min. Sci. 50, 508–526. https://doi.org/10.1134/S1062739114030132.

Moreira, C.A., Borssatto, K., Ilha, L.M., Santos, S.F., Rosa, F.T.G., 2016. Geophysical modeling in gold deposit through DC Resistivity and Induced Polarization methods. REM - Int. Eng. J. 69, 293–299. https://doi.org/10.1590/0370-44672016690001.

Moses, D., Shimada, H., Sasaoka, T., Hamanaka, A., Dintwe, T.K., Wahyudi, S., 2020. Rock Slope Stability Analysis by Using Integrated Approach. World J. Eng. Technol. 8, 405–428. https://doi.org/10.4236/wjet.2020.83031.

Rahimi, E., Moosavi, E., Shirinabadi, R., Gholinejad, M., 2018. Optimized algorithm in mine production planning, mined material destination, and ultimate pit limit [J]. J. Cent. South Univ. 25 (6), 1475–1488. https://doi.org/10.1007/s11771-018-3841-5.

Rahmanpour, M., Osanloo, M., 2017. A decision support system for determination of a sustainable pit limit. J. Clean. Prod. 141, 1249–1258. https://doi.org/10.1016/j.jclepro.2016.09.205.

Samavati, M., Essam, D., Nehring, M., Sarker, R., 2018. A new methodology for the open-pit mine production scheduling problem. Omega (United Kingdom) 81, 169–182. https://doi.org/10.1016/j.omega.2017.10.008.

Silva, P.C.S., Yamato, A.A., Vasconcelos, C.S., Lopes, I., 1999. Curitiba - Folha SG.22-X-D-I. See. https://rigeo.cprm.gov.br/handle/doc/8486.

Silva, A.D.R., Campos, F.F., Brumatti, M., Salvador, E.D., Pavan, M., 2019. Mineralizações Polimetálicas (Pb-Zn-Ag-Cu-Ba) associadas à Formação Perau. Cinturão Ribeira Meridional. http://rigeo.cprm.gov.br/jspui/handle/doc/21258.

Thornton, R., 2014. Zamazama, "illegal" artisanal miners, misrepresented by the South African Press and Government. Extr. Ind. Soc. 1, 127–129. https://doi.org/10.1016/J.EXIS.2014.06.003.

Vieira, O.A.R.P., Godoy, A.M., Hackspacher, P.C., Júnior, W.B.L., 2018. Contexto estrutural da área da folha topográfica Guapiara. Geosciences= Geociências. 37 (3), 505–521. https://doi.org/10.5016/geociencias.v37i3.12532.

Yang, C.-H., Cheng, P.-H., You, J.-I., Tsai, L.L., 2002. Significant resistivity changes in the fault zone associated with the 1999 Chi-Chi earthquake, west-Central Taiwan. Tectonophysics 350, 299–313. https://doi.org/10.1016/S0040-1951(02)00146-4.

Zarroca, M., Linares, R., Velásquez-López, P.C., Roqué, C., Rodríguez, R., 2015. Application of electrical resistivity imaging (ERI) to a tailings dam project for artisanal and small-scale gold mining in Zaruma-Portovelo. Ecuador. J. Appl. Geophys. 113, 103–113. https://doi.org/10.1016/J.JAPPGEO.2014.11.022.

Zhang, Q., Zhu, H., 2018. Collaborative 3D geological modeling analysis based on multi-source data standard. Eng. Geol. 246, 233–244. https://doi.org/10.1016/J.ENGGEO.2018.10.001.

Zvarivadza, T., Nhleko, A.S., 2018. Resolving artisanal and small-scale mining challenges: moving from conflict to cooperation for sustainability in mine planning. Res. Policy 56, 78–86. https://doi.org/10.1016/J.RESOURPOL.2017.12.003.